JVSTB
Journal of Vacuum Science & Technology B

Practical approach to modeling e-beam lithographic process from SEM images for minimization of line edge roughness and critical dimension error

Rui Guo, Soo-Young Lee, Jin Choi, Sung-Hoon Park, In-Kyun Shin, and Chan-Uk Jeon

Citation: Journal of Vacuum Science & Technology B **34**, 011601 (2016); doi: 10.1116/1.4937740
View online: http://dx.doi.org/10.1116/1.4937740
View Table of Contents: http://scitation.aip.org/content/avs/journal/jvstb/34/1?ver=pdfcov
Published by the AVS: Science & Technology of Materials, Interfaces, and Processing

Articles you may be interested in

Analytic estimation and minimization of line edge roughness in electron-beam lithography
J. Vac. Sci. Technol. B **33**, 06FD07 (2015); 10.1116/1.4936070

Minimization of line edge roughness and critical dimension error in electron-beam lithography
J. Vac. Sci. Technol. B **32**, 06F505 (2014); 10.1116/1.4899238

Temperature dependent effective process blur and its impact on exposure latitude and lithographic targets using e-beam simulation and proximity effect correction
J. Vac. Sci. Technol. B **32**, 06F503 (2014); 10.1116/1.4896600

Derivation of line edge roughness based on analytic model of stochastic exposure distribution
J. Vac. Sci. Technol. B **31**, 06F408 (2013); 10.1116/1.4827816

Fabrication of a Fresnel zone plate through electron beam lithographic process and its application to measuring of critical dimension scanning electron microscope performance
J. Vac. Sci. Technol. B **25**, 1771 (2007); 10.1116/1.2787874

SHIMADZU
Excellence in Science
Powerful, Multi-functional UV-Vis-NIR and FTIR Spectrophotometers
Providing the utmost in sensitivity, accuracy and resolution for a wide array of applications in materials characterization and nanotechnology research
• Photovoltaics • Ceramics
• Polymers • FPDs
• Thin films • Coatings
• Paints/inks • Semiconductors
Click here to learn more

Redistribution subject to AVS license or copyright; see http://scitation.aip.org/termsconditions. IP: 131.204.73.184 On: Thu, 07 Apr 2016 01:29:43

CrossMark

Practical approach to modeling e-beam lithographic process from SEM images for minimization of line edge roughness and critical dimension error

Rui Guo and Soo-Young Lee[a)]
Department of Electrical and Computer Engineering, Auburn University, Auburn, Alabama 36849

Jin Choi, Sung-Hoon Park, In-Kyun Shin, and Chan-Uk Jeon
Samsung Electronics, Photomask Division, 16 Banwol-Dong, Hwasung, Kyunggi-Do 445-701, Korea

(Received 28 June 2015; accepted 1 December 2015; published 16 December 2015)

Two main factors which limit the minimum feature size and the maximum circuit density achievable by electron-beam (e-beam) lithography are the line edge roughness (LER) and the proximity effect. Since the LER is caused by the stochastic nature of the exposing and development processes, it does not scale with the feature size. Therefore, reducing the LER is essential as the feature size continues to decrease. Accurate modeling of the LER and the proximity effect analytically or via simulation for their minimization is either difficult or costly in many cases. In this study, a practical method for extracting the essential information from SEM images, needed to characterize the e-beam lithographic process, and an effective method for minimizing the LER and critical dimension error based on the extracted information have been developed. The main objective is that the methods utilize only the information extracted from SEM images without having to know the complete setup of e-beam lithographic process. It has been shown that they have a good potential to be further developed into practical and useful tools. © *2015 American Vacuum Society.*
[http://dx.doi.org/10.1116/1.4937740]

I. INTRODUCTION

One of the main issues in the electron-beam (e-beam) lithography is the proximity effect caused by electron scattering. Effective proximity effect correction schemes have been developed and implemented by many researchers.[1–5] As the feature size continues to decrease,[6] the line edge roughness (LER) has become an unavoidable problem to deal with since it does not scale with the feature size. Therefore, both the proximity effect and the LER must be considered in an effort to minimize the feature size in a pattern of nanoscale features.

Most of the efforts to model or reduce the LER and proximity effect in the past were made through an analytic, simulation, or experimental method.[7–10] It is not uncommon that the results optimized by the analytic and simulation methods are substantially different from the actual experimental results. This difference may be due to the particular model employed, the assumptions made, and the phenomena ignored. For example, in our previous study,[11] a computational approach to minimizing the LER was taken. Two methods developed for the LER minimization are based on the results obtained through the Monte Carlo (MC) and development simulations. However, since the MC and development simulations may not capture completely all the characteristics of the e-beam lithographic process, their results may not be very realistic. Also, an experimental method with a trial-and-error approach would be costly due to the repeated experiments.

In this study, an attempt to develop methods which are practical and realistic in reducing the proximity effect and LER has been made. The essential information for modeling the e-beam lithographic process, i.e., modeling (estimating) the line spread function (LSF), the conversion [from the exposure (energy deposited in the resist) to the developing rate] formula, and the (stochastic) exposure fluctuation, is extracted through analyzing SEM images. Based on the modeled e-beam lithographic process, the critical dimension (CD) error and LER are minimized through an optimization procedure. The CD error is defined as the difference between the target and actual edge locations. In the modeling, only the information from SEM images is utilized with the assumption that each SEM image is an accurate representation of the corresponding resist profile, and no knowledge on the experimental setup other than the relative dose levels is required. Through iterations, the difference between the modeled and measured resist profiles is minimized (the *modeled resist profile* refers to the resist profile obtained using the modeled LSF, conversion formula and exposure fluctuation). Since the proposed methods utilize the experimental results of SEM images directly, their results are likely to be realistic. Another important aspect of the proposed methods is that the LSF, conversion formula, and exposure fluctuation are modeled together rather than individually. Therefore, a minor inaccuracy in one of them may be compensated by the others such that the modeled resist profile with high accuracy can still be achieved. As a first step, the proposed methods have been implemented for patterns of long lines. In this paper, the methods are described in detail with the early experimental results.

The rest of the paper is organized as follows. The preprocessing of SEM images and the edge detection are described in Sec. II. The modeling of e-beam lithographic process is described in Sec. III. The minimization method is presented

a)Electronic mail: leesooy@eng.auburn.edu

Redistribution subject to AVS license or copyright; see http://scitation.aip.org/termsconditions. IP: 131.204.73.184 On: Thu, 07 Apr 2016 01:29:43

in Sec. IV. The results of modeling SEM images and minimizing the LER and CD error are discussed in Sec. V, followed by a summary in Sec. VI.

II. ANALYSIS OF SEM IMAGES

A typical substrate system is assumed, where a resist layer with a certain thickness is on top of the substrate. A pattern of multiple long lines is exposed with different levels of a uniform dose, while all the other e-beam lithographic parameters, i.e., beam energy, developing time, etc., are fixed. After the resist development process, SEM images are taken in a top-down view of the remaining resist profile. An example of such a SEM image is shown in Fig. 1, to be used in illustrating the steps of analyzing SEM images. Using image processing techniques, the feature boundaries (edges) are detected to measure the CD (linewidth) and LER.

A. Preprocessing

SEM images typically include a significant level of "salt and pepper" noise (see Fig. 1), and their quality, e.g., brightness or contrast, may vary from image to image or spatially within an image. Since the proposed methods utilize the information (CD and LER) extracted from SEM images, it is important to reduce the noise level and enhance the image quality.

A spatial-averaging filter such as Gaussian filter reduces the noise level but at the same time tends to smooth out the image detail such as roughness of feature boundary. Also, it is not very effective on the salt-and-pepper noise. On the other hand, the median filter is effective in reducing the salt-and-pepper noise without destroying the image detail significantly. Therefore, the median filter is employed in this study. The larger the size of the median filter is, the more image detail can be lost. The smallest size of the median filter which removes most of the discontinuity of the detected edges is found to be 9×9 pixels (12.6×12.6 nm). The SEM image (Fig. 1) after the noise reduction is shown in Fig. 2(a).

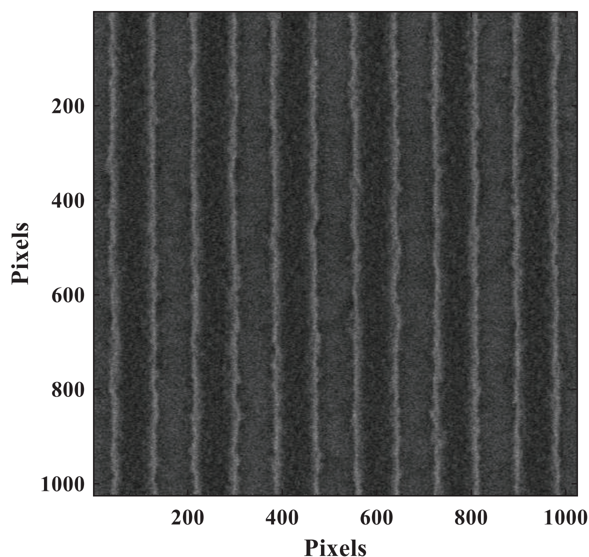

Fig. 1. Example of SEM images taken in the top-down view of remaining resist profile.

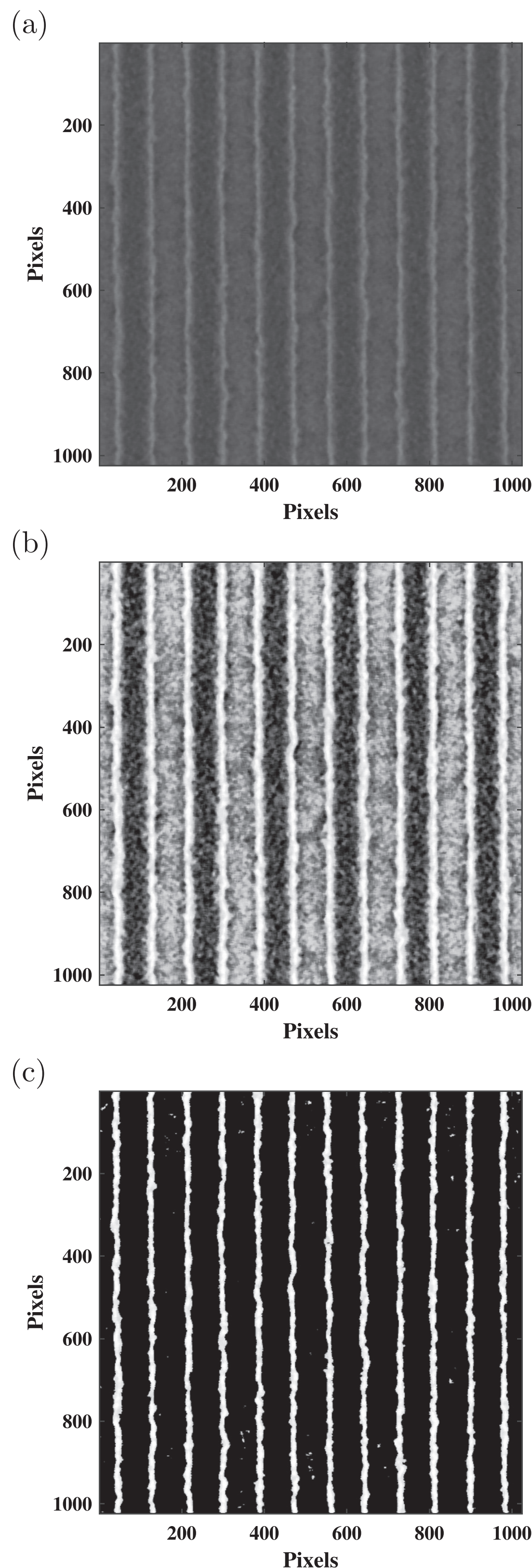

Fig. 2. SEM images preprocessed for (a) noise reduction, (b) contrast enhancement, and (c) background removal.

Redistribution subject to AVS license or copyright; see http://scitation.aip.org/termsconditions. IP: 131.204.73.184 On: Thu, 07 Apr 2016 01:29:43

Since the boundary detection is based on the change in brightness, a SEM image with a low contrast is prone to a detection error. The contrast of such image is enhanced by a histogram equalizer for better detection. The result of contrast enhancement is shown in Fig. 2(b). The contrast enhancement is carried out after the noise reduction not to increase the noise level.

B. Detection of feature boundaries

In SEM images, boundary (edge) regions are brighter than the background. To facilitate detecting the feature boundaries, the background is removed by using a threshold, as shown in Fig. 2(c). However, some small regions not in the edge regions may have a brightness higher than the threshold and survive the thresholding (see Fig. 3). Therefore, a window centered at each peak of brightness is employed to define the edge region, and any area outside the edge regions is set to be zero.

A 3×3 differential edge detector is employed (laterally) in edge regions, to obtain the gradient of the preprocessed SEM images. The maximum positive and negative gradients are searched to find the inner and outer edge locations [see Fig. 4(b)]. The feature boundaries are normally continuous in space. Isolated edges such as a single pixel of edge are most probably due to the salt-and-pepper noise and therefore are removed. In Fig. 4(a), the detected edges are overlaid with the original image, where a high-fidelity result can be observed.

The outer and inner edges shown in Fig. 4(b) may correspond to the edges at the top and bottom layers of resist, respectively, in the case of an overcut resist profile. In the current implementation, both inner and outer edges are considered to utilize as much information extracted from SEM images as possible in the modeling process, specifically matching the linewidth. However, an alternative is to use the average edge location, e.g., the average of the inner and outer edge locations, or detecting the peak brightness (instead of the maximum gradient) in the edge region.

The average inner and outer linewidths are computed from the inner and outer edge locations, and the LER is evaluated as the standard deviation of the inner and outer edge locations, i.e., 1–σ LER. The orientation of lines may not be perfectly aligned with the axes of the SEM imaging system. The tilt angle is estimated using the method of image moments and is compensated in measuring the linewidth and LER. The average inner and outer linewidths and LERs measured from the SEM images with four different normalized dose levels (from 0.705 to 1.082) are plotted in Fig. 5. The proposed methods do not require the absolute doses to be known, and the normalized dose is used only to distinguish different doses, i.e., relative dose levels, and the normalized dose of 1.0 does not have any special meaning.

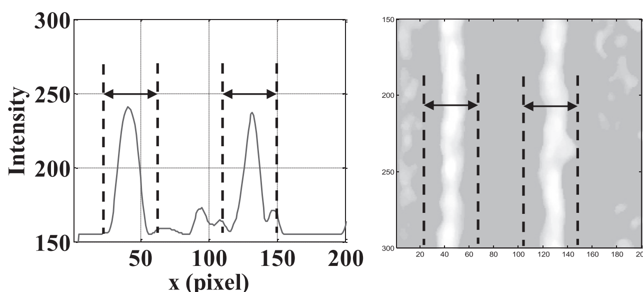

FIG. 3. Edge region defined by a window centered at the peak brightness.

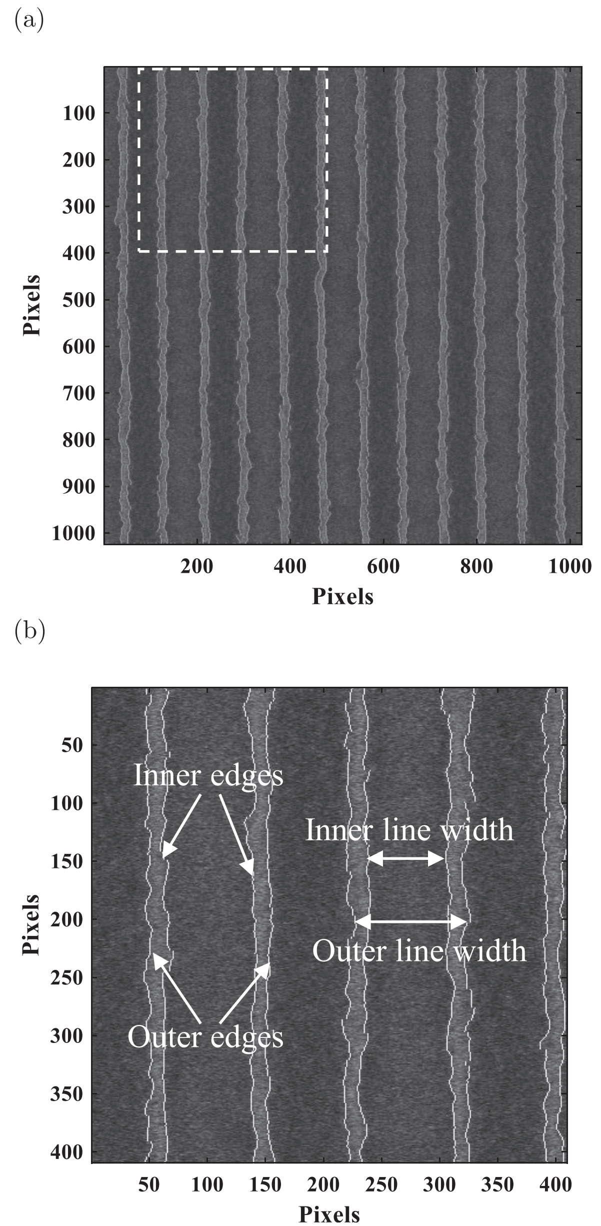

FIG. 4. (a) Detected edges are overlaid with the original SEM image and (b) a zoomed-in region [the white box shown in (a)] where inner and outer edges are illustrated.

III. MODELING OF E-BEAM LITHOGRAPHIC PROCESS

In this section, the procedures for modeling the e-beam lithographic process, i.e., estimating the LSF, the conversion formula, and the exposure fluctuation based on the linewidth and LER measured from SEM images are described. Note

Redistribution subject to AVS license or copyright; see http://scitation.aip.org/termsconditions. IP: 131.204.73.184 On: Thu, 07 Apr 2016 01:29:43

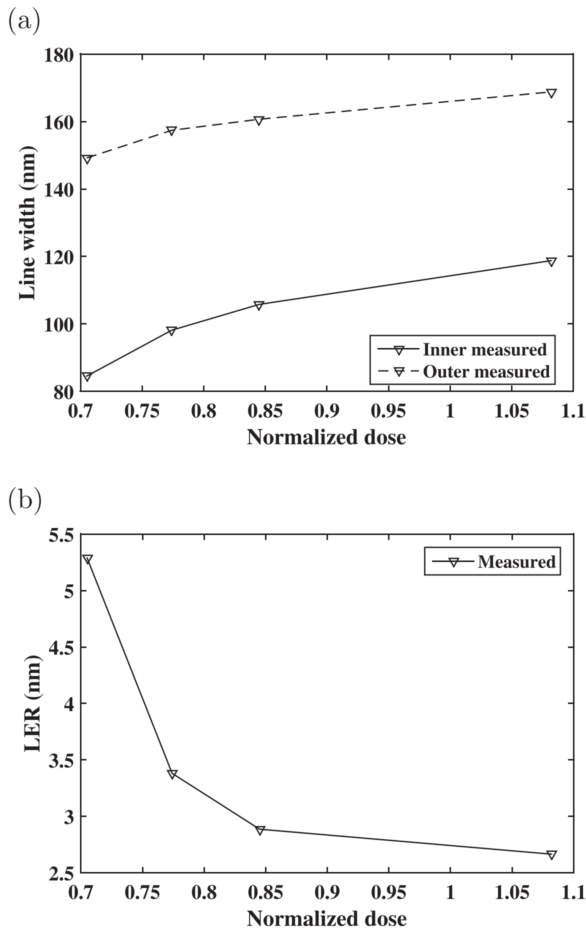

FIG. 5. (a) Inner and outer linewidths and (b) the LER measured from a set of SEM images.

that the proximity effect and LER are reflected in the LSF and exposure fluctuation, respectively. In the proposed methods, the LSF, conversion formula, and exposure fluctuation are modeled together rather than individually. This approach allows a modeling error in one to be compensated in the others as long as the modeled linewidth and LER closely match with the measured ones. Also, the approach makes it unnecessary to know certain experimental details such as the absolute dose and developing time. For example, through the modeling process, the LSF and conversion formula adapt themselves to an assumed developing time. In other words, the final outcomes, e.g., the normalized dose and line-width reduction optimized by the proposed methods, are independent of the assumed developing time.

A. Development model

In this study, only the line/space patterns are considered, and therefore, the exposure distribution in the resist can be computed using the LSF, which describes the exposure distribution when an infinitely long line with the single-pixel width is exposed. Assuming that each line is long in the Y-dimension (refer to Fig. 9), the LSF is expressed as $lsf(x, z)$. Then, the 3D spatial distribution of exposure $e(x, y, z)$ at point (x, y, z) in the resist can be computed by the following convolution:

$$e(x,y,z) = \int p(x-x',0)\,lsf(x',z)\,dx'. \quad (1)$$

In the above equation, $p(x, 0)$ represents the spatial dose distribution

$$p(x,0) = \begin{cases} D & \text{within each feature} \\ 0 & \text{otherwise,} \end{cases} \quad (2)$$

where D is a uniform dose.

Most resists are nonlinear, i.e., the developing rate is not linearly proportional to the exposure. Therefore, a nonlinear function, referred to as conversion formula, may be employed to describe the relationship between the exposure and developing rate. That is, the exposure $e(x, y, z)$ is converted into the developing rate $r(x, y, z)$ through the conversion formula. The conversion formula is a monotonically increasing function, and its typical shape may be modeled by the function in Eq. (3) where only the portion of the curve before its peak is used. The validity of this form of function used as a conversion formula was verified through experiment in an earlier study[12]

$$r(x,y,z) = k_1 \cdot \exp\left(-\frac{\left(e(x,y,z)-k_2\right)^2}{k_3}\right) + k_4. \quad (3)$$

In Eq. (3), $k_1 + k_4$ represents the maximum developing rate, k_2 corresponds to the lowest exposure leading the maximum developing rate, k_3 describes the rate contrast with respect to the exposure, and k_4 is the minimum developing rate for a nonzero exposure. Through the modeling process, the parameters $\{k_i\}$ are determined.

In the modeling process, the estimated resist profile is compared with the measured profile from SEM images, and the difference between them is minimized. The estimated resist profile is obtained from the distribution of developing rate, $r(x, y, z)$, using the path-based simulation method[12] previously developed. In the path-based method, the resist development process is modeled by L-shape development paths starting from the resist surface toward the boundaries of the (remaining) resist profile. Each path consists of a vertical path segment (representing vertical development) and lateral path segments (representing lateral development). Given a developing time, all possible paths are traced without iterations, and the remaining resist profile is determined by those paths reaching the farthest points.

B. Matching linewidth

In the first step, the LSF and conversion formula are modeled utilizing the information extracted from the SEM images of different (normalized) doses, specifically, matching the average inner and outer linewidths obtained using the modeled LSF and conversion formula to those measured from the SEM images. An iterative procedure is employed, i.e., the LSF and the conversion formula are adjusted through iterations, such that the total difference between the modeled and measured average inner and outer linewidths is

Redistribution subject to AVS license or copyright; see http://scitation.aip.org/termsconditions. IP: 131.204.73.184 On: Thu, 07 Apr 2016 01:29:43

minimized. The total difference refers to the sum of the differences for all SEM images. The iterative procedure is described below and also illustrated in Fig. 6.

Step 1: Adjust one of the parameters (k'_i) in the conversion formula each time.
Step 2: Adjust each point of the LSF.
Step 3: Compute the exposure distribution through the convolution of the LSF with the dose distribution.
Step 4: Compute the developing rate distribution.
Step 5: Perform the resist development simulation.
Step 6: Calculate the total difference between the modeled and measured average inner and outer linewidths.
Step 7: Check whether the total difference is acceptable. If yes, stop the iteration. Otherwise go to step 8.
Step 8: Check whether the total difference can be reduced by further adjusting the LSF. If yes, go to step 2. Otherwise, go to step 1.

In adjusting the conversion formula, the following constraints are imposed: the k'_is are positive, and the conversion formula is a monotonically increasing function. Also, the following constraints are imposed on adjusting the LSF (see Fig. 7):

(1) The LSF is adjusted point-wise from the center to the outside iteratively until the local optimal value is found for each point.
(2) All the previous points are set slightly lower than their optimal values so that the following points have more room to be adjusted.
(3) Each adjustment is linearly proportional to the current total difference, since a larger difference usually requires more adjustment.
(4) The current point of LSF is always set smaller than the previous points, since the LSF is a monotonously decreasing function.

Since both the LSF and the conversion formula affect the average inner and outer linewidth, the total difference is minimized when both of them are optimized. The examples of the modeled LSF and the conversion formula are shown in Fig. 8.

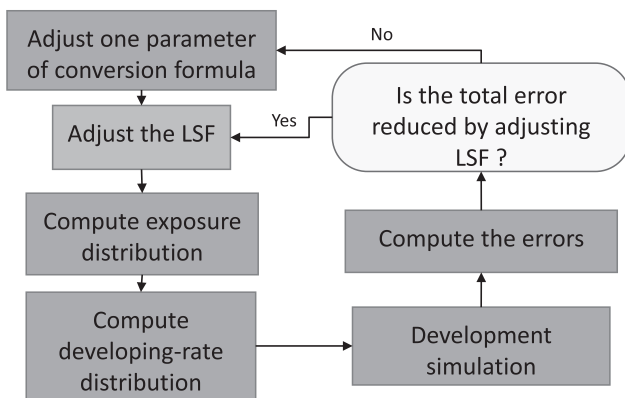

Fig. 6. Flowchart of the iterative procedure for determining the conversion formula (and the LSF).

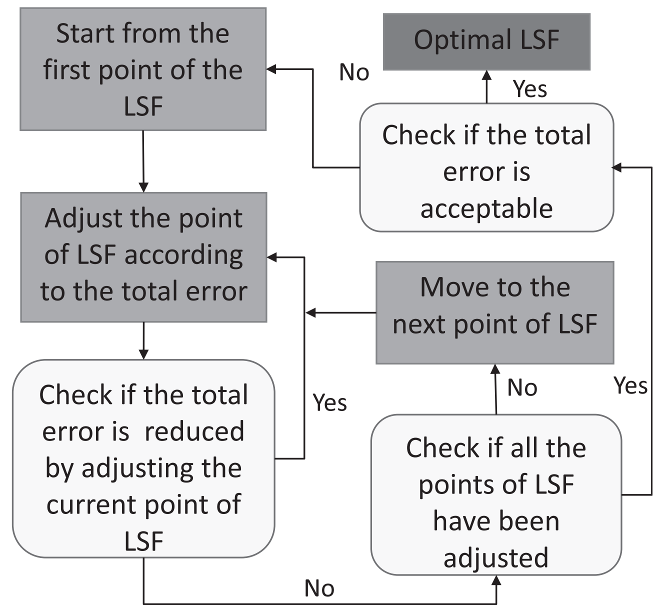

Fig. 7. Flowchart of the iterative procedure for adjusting each point of the LSF.

C. Matching the LER

In the second step, the (stochastic) fluctuation of exposure is modeled by matching the LER values obtained from the modeled exposure fluctuation to those measured

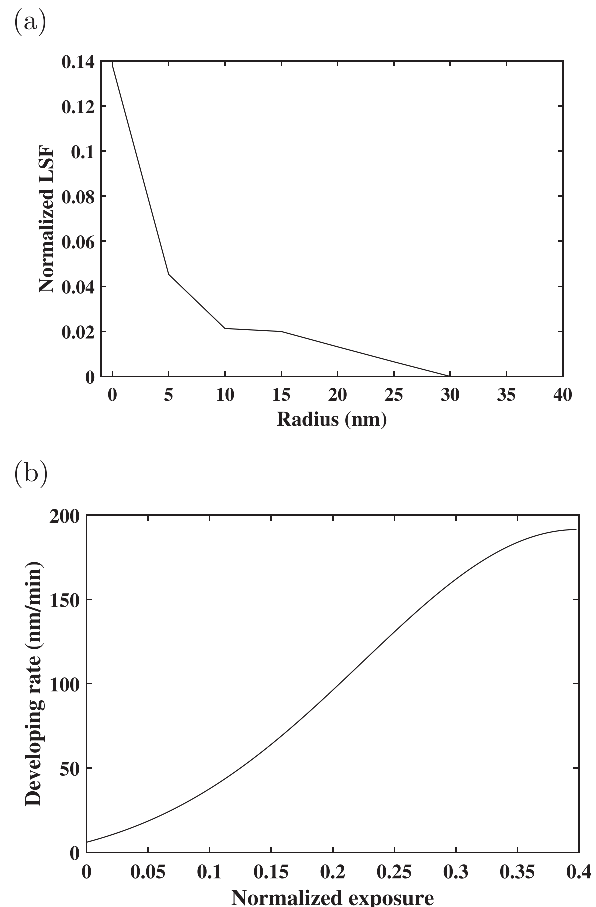

Fig. 8. (a) LSF and (b) the conversion formula derived.

Redistribution subject to AVS license or copyright; see http://scitation.aip.org/termsconditions. IP: 131.204.73.184 On: Thu, 07 Apr 2016 01:29:43

in the SEM images. The LER is caused by a number of stochastically fluctuating effects such as shot noise, distributions of chemical species in the resist such as photoacid generator (PAG), resist development process, etc.[11,13] Such fluctuations can be reflected in the developing rate. Through the conversion formula, the fluctuation of developing rate can be converted into the fluctuation of exposure. Since the Poisson process is to model most particle processes, i.e., shot noise and electron scattering, a zero-mean Poisson noise, $e_n(x, y, z)$, is added to the (deterministic) exposure, $e_d(x, y, z)$, to model the fluctuation of exposure as follows:

$$e_s(x,y,z) = e_d(x,y,z) + e_n(x,y,z),$$
$$e_n(x,y,z) \sim (\text{Poisson}(\lambda) - \lambda) * \sigma_n(x,y,z),$$

where $e_s(x, y, z)$ represents the stochastic exposure and $\sigma_n(x, y, z)$ determines the level of exposure fluctuation.

Assuming that the exposure fluctuation is an uncorrelated stochastic process, a higher exposure level leads to a higher absolute fluctuation, but a lower relative fluctuation. These properties are incorporated into the implementation of exposure fluctuation as in Eq. (4)

$$\sigma_n(x,y,z) = \sigma_0\left(\frac{e_d(x,y,z)}{\max(e_d(x,y,z))}\right)^{\alpha}, \quad (4)$$

where $0 < \alpha < 1$ and max() is the maximum operator.

It can be seen in Eq. (4) that as the exposure level [$e_d(x, y, z)$] increases, the absolute fluctuation $\sigma_n(x, y, z)$ becomes larger, but the relative fluctuation, defined as $\sigma_n(x,y,z)/e_d(x,y,z)$, becomes smaller. The two parameters, σ_0 and α, are determined through an iterative procedure (the similar procedure as for matching the linewidth) such that the total difference between the modeled and measured LERs is minimized. Note that the added fluctuation of exposure may also affect matching the linewidth. Therefore, the two procedures, matching the linewidth and matching the LER, are alternated to minimize the recursive effect between them. The final outcomes of modeling are the LSF, conversion formula, and exposure fluctuation, which closely match the modeled linewidths and LERs to those measured from the SEM images, and are used in minimizing the LER and CD error.

IV. MINIMIZATION OF LER AND CD ERROR

In a previous study,[14] it is observed that the LER is high inside a feature, rapidly decreases over the feature edge, and then mostly stays low or slightly increases outside the feature. This is mainly due to the fact that the exposure level quickly drops down from the exposed area (inside the feature) to the unexposed area (outside the feature) and the absolute stochastic fluctuation of exposure is smaller outside the feature, i.e., in the unexposed area. These behaviors indicate that it might be possible to reduce the LER by shrinking the area of a feature to be exposed, from the feature boundary inward. Based on this observation, the shape control method was developed earlier,[11] which reduces the area to be exposed by ΔW on each side of the feature, instead of exposing the whole feature, as illustrated in Fig. 9. This approach of shape control is employed in this study.

It is not possible to minimize the LER and CD error individually (since the LER may not be minimal when the CD error is minimized). Also, it may not be always possible to reduce both the LER and CD error in each step of the minimization. Therefore, a cost function consisting of the LER and CD error is employed

$$C(x) = \text{CD error} + 3\,\text{LER}. \quad (5)$$

As defined earlier, the CD error is the difference between the target and actual edge locations, averaged over the inner and outer edge locations. The LER is defined as the standard deviation of edge location (i.e., $1\text{–}\sigma$ LER). Hence, the cost function of CD error + 3 LER is very close to the worst case deviation of edge location from the target location (e.g., 99.7% in the case of Gaussian distribution). Also, 3 LER corresponds to the $3\text{–}\sigma$ LER typically used in the research and industry communities.

The optimal amount of line-width reduction, $2\Delta W$, and the dose, which minimizes the cost function, are determined through an iterative procedure. In each iteration, ΔW is increased by a small amount, and the feature area to be exposed is reduced by ΔW on each side of the feature. Then, the total dose is adjusted so that the cost function is minimized. The iteration continues until the cost function cannot be reduced any further.

V. RESULTS AND DISCUSSION

Two sets of SEM images obtained under the same experimental setup (except the dose) are used in the modeling and minimization. The first set includes four SEM images corresponding to the four normalized dose levels of 0.845, 0.920, 1.000, and 1.082 where both the linewidth and space are 60 nm. The other set includes four SEM images corresponding to the four normalized dose levels of 0.705, 0.774, 0.845, and 1.082 where both the linewidth and space are 120 nm. The beam energy is 50 keV. Other details of experiment are

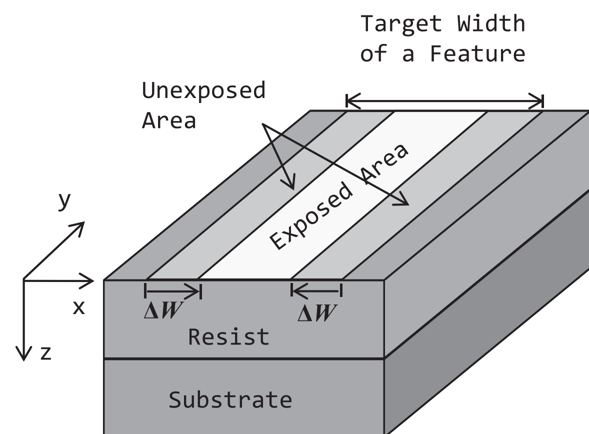

FIG. 9. In the shape control method, the feature area is reduced with the dose increased.

Redistribution subject to AVS license or copyright; see http://scitation.aip.org/termsconditions. IP: 131.204.73.184 On: Thu, 07 Apr 2016 01:29:43

confidential outside Samsung at the time of writing this paper.

In order to minimize the statistical uncertainty of the result, all of the lines in each SEM image are utilized in measuring the linewidth (edge locations) and LER, 12 lines in the pattern of 60 nm lines and six lines in the pattern of 120 nm lines. Using the Student's t-distribution, the 90% confidence interval is computed for each of the CD error and LER measurements.

The linewidth and LER obtained by the proposed modeling method are compared with those measured from the SEM images for the 60 nm line pattern in Fig. 10. It can be seen that the modeled linewidth and LER are closely matched with the measured results. A similar close match can be observed for the 120 nm line pattern in Fig. 11.

Furthermore, the minimizations of the LER and CD error based on the modeling results are shown in Fig. 12. By increasing the amount of ΔW, the cost function is reduced and eventually reaches to the minimum, where the optimal dose changes with ΔW.

In Fig. 13, the experimental results, SEM images, obtained using the optimal ΔW and dose determined by the shape control method, are compared with the results obtained without the shape control. It needs to be pointed out that the "results without the shape control" refer to the SEM images used in the modeling, i.e., they are not the optimized results. For the 60 nm-line pattern, the 1-σ LER is reduced from 3.25 nm (90% confidence interval: [3.17, 3.33] nm) to 3.10 nm (90% confidence interval: [3.02, 3.18] nm) and the CD error decreases from 6.07 nm (90% confidence interval: [6.03, 6.11] nm) to 0.46 nm (90% confidence interval: [0.41, 0.51] nm). For the 120 nm-line pattern, the 1-σ LER is reduced from 3.38 nm (90% confidence interval: [3.22, 3.54] nm) to 2.93 nm (90% confidence interval: [2.77, 3.08] nm) and the CD error decreases from 3.67 nm (90% confidence interval: [3.62, 3.72] nm) to 0.64 nm (90% confidence interval: [0.59, 0.69] nm). For the 120 nm-line pattern, both CD error and LER have been reduced significantly by the shape control method. In the case of the 60 nm-line pattern, the CD error has been greatly reduced, but the LER reduction is marginal. However, the line edges with the shape control look visibly less rough than those without the shape control [compare Figs. 13(a) and 13(b)].

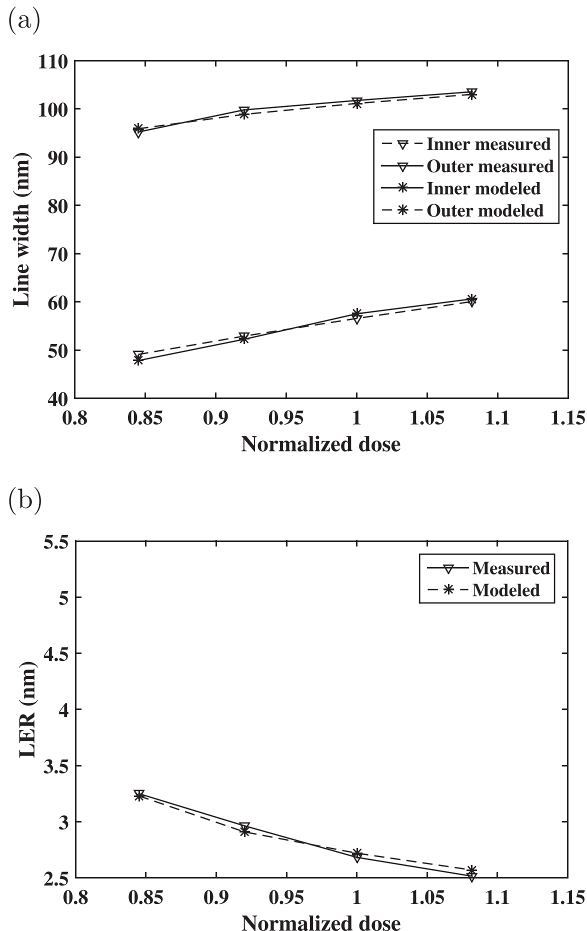

FIG. 10. Linewidth and LER modeled through simulation are compared with those measured from the SEM images of line pattern with L = S = 60 nm: (a) average linewidth (inner and outer) and (b) LER.

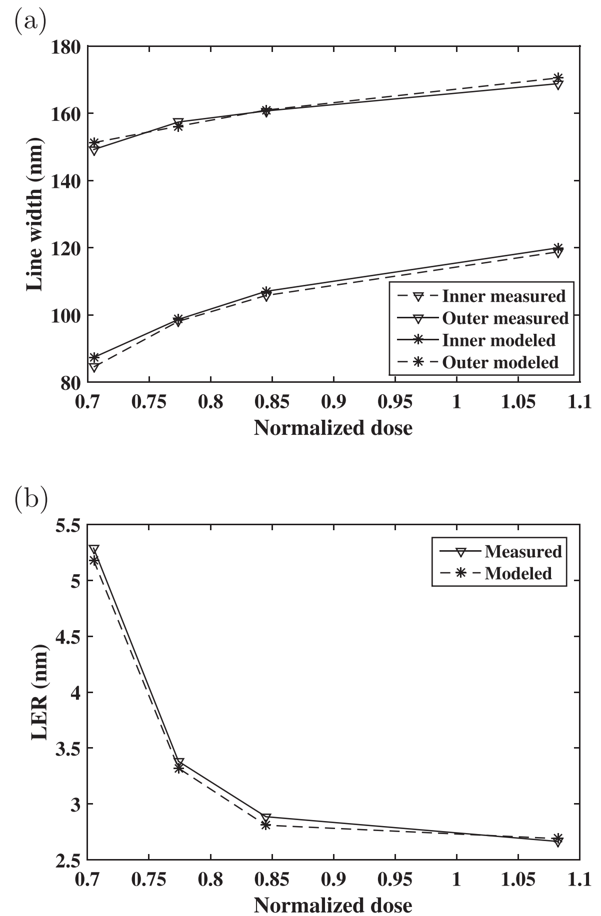

FIG. 11. Linewidth and LER modeled through simulation are compared with those measured from the SEM images of line pattern with L = S = 120 nm: (a) average linewidth (inner and outer) and (b) LER.

VI. SUMMARY

In this study, a practical method for accurately matching the modeled line-width and LER to those measured from SEM images has been developed. The main objective is that

Redistribution subject to AVS license or copyright; see http://scitation.aip.org/termsconditions. IP: 131.204.73.184 On: Thu, 07 Apr 2016 01:29:43

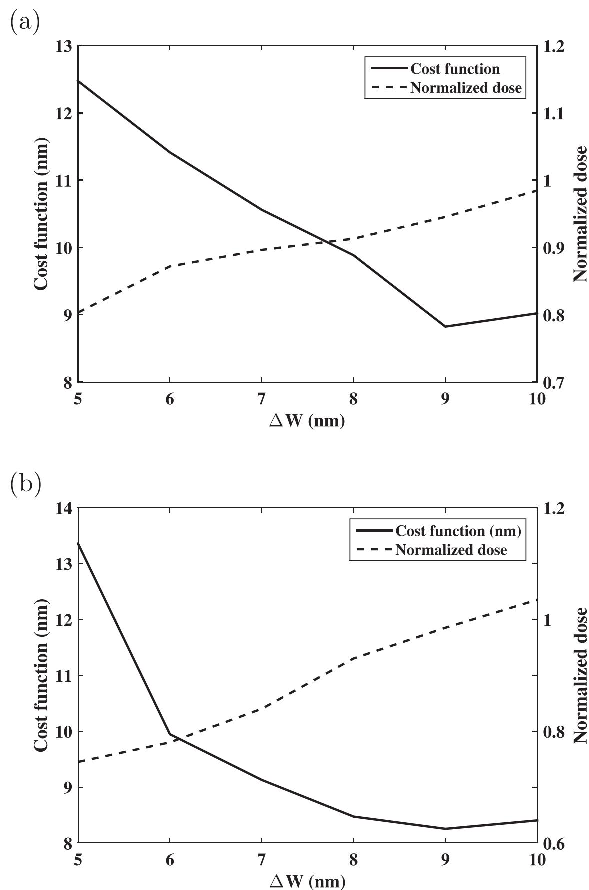

FIG. 12. Minimized cost function and respective normalized dose: (a) L = S = 60 nm and (b) L = S = 120 nm.

the method utilizes only the information extracted from SEM images with the normalized dose levels without having to know the complete setup of e-beam lithographic process. Also, an effective method for minimizing the LER and CD error based on the modeling results has been implemented. It has been shown that the results obtained from the modeling method are closely matched with those measured from the SEM images, and the minimization method reduces the LER and CD error substantially. Since only the information extracted from the SEM images is required, the proposed methods may have a potential to be further developed into practical tools, which are widely applicable and able to generate realistic results.

Nevertheless, few points are worthwhile to be pointed out about the (current implementations of) methods. First, the methods assume that each SEM image is an accurate representation of the corresponding resist profile. Any substantial distortion in SEM images can lead to an error in the modeling and minimization, and therefore, it is critical to obtain a set of SEM images with a minimal distortion. Second, the quality of SEM images can affect the accuracy of results. It is important to enhance the image quality such as the signal-to-noise ratio and image contrast as much as possible through the preprocessing of images. The image processing techniques employed in this study must have room for improvement. Third, the methods consider only the patterns of lines/spaces and needs to be extended to be able to handle other shapes of features. Since the point spread function can be derived from the LSF, it is expected that the methods can be further developed for more general patterns.

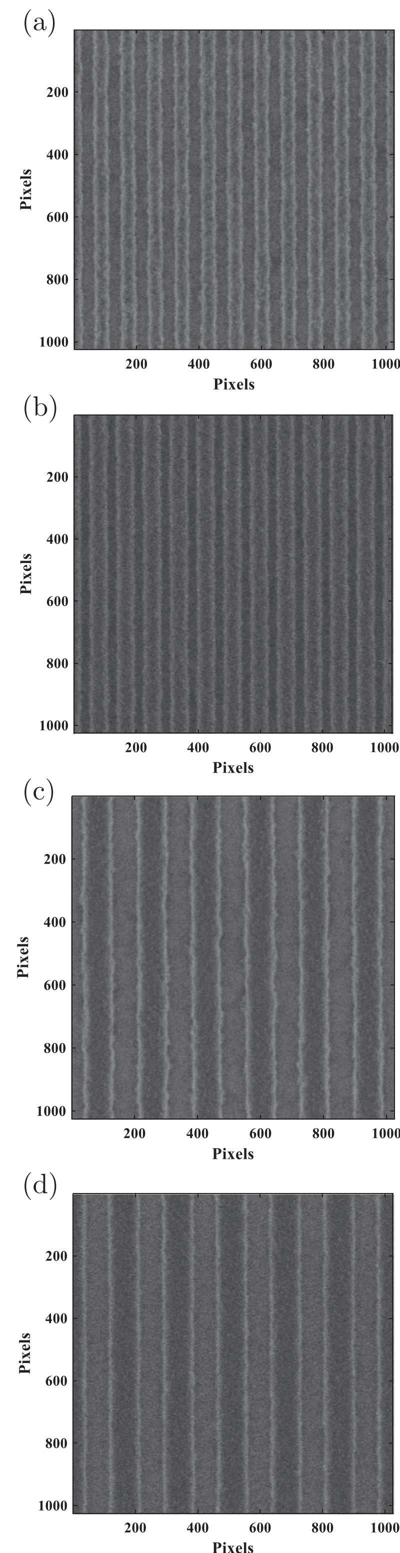

FIG. 13. SEM images of remaining resist profiles: (a) without the shape control, L = S = 60 nm, (b) with the shape control applied, L = S = 60 nm, $\Delta W = 5$ nm, the normalized dose = 0.926, (c) without the shape control, L = S = 120 nm, and (d) with the shape control applied, L = S = 120 nm, $\Delta W = 5$ nm, the normalized dose = 0.980.

Redistribution subject to AVS license or copyright; see http://scitation.aip.org/termsconditions. IP: 131.204.73.184 On: Thu, 07 Apr 2016 01:29:43

Lastly, the methods use only the information extracted from SEM images. By utilizing additional information on the e-beam lithographic process, which is available, the methods may be simplified and their accuracy may be improved. Some of these points will be considered in the future study.

ACKNOWLEDGMENT

This work was supported by a research grant from Samsung Electronics Co., Ltd.

[1]H. Eisenmann, T. Waas, and H. Hartmann, J. Vac. Sci. Technol., B **11**, 2741 (1993).
[2]S.-Y. Lee and B. D. Cook, IEEE Trans. Semicond. Manuf. **11**, 108 (1998).
[3]M. Osawa, K. Takahashi, M. Sato, and H. Arimoto, J. Vac. Sci. Technol. B **19**, 2483 (2001).
[4]Q. Dai, S.-Y. Lee, S.-H. Lee, B.-G. Kim, and H.-K. Cho, Microelectron. Eng. **88**, 902 (2011).
[5]Q. Dai, S.-Y. Lee, S.-H. Lee, B.-G. Kim, and H.-K. Cho, J. Vac. Sci. Technol. B **30**, 06F307 (2012).
[6]M. Nagase, H. Namatsu, K. Kurihara, K. Iwadate, K. Murase, and T. Makino, Jpn. J. Appl. Phys. **35**, 4166 (1996).
[7]G. P. Patsis, N. Tsikrikas, D. Drygiannakis, and I. Raptis, Microelectron. Eng. **87**, 1575 (2010).
[8]Z. Yu, L. Chen, W. Wu, H. Ge, and S. Y. Chou, J. Vac. Sci. Technol. B **21**, 2089 (2003).
[9]Y. Ma, G. Tsvid, and F. Cerrina, J. Vac. Sci. Technol. B **21**, 3124 (2003).
[10]R. Guo, S.-Y. Lee, J. Choi, S.-H. Lee, I.-K. Shin, C.-U. Jeon, B.-G. Kim, and H.-K. Cho, J. Vac. Sci. Technol. B **31**, 06F408 (2013).
[11]X. Zhao, S.-Y. Lee, J. Choi, S.-H. Lee, I.-K. Shin, and C.-U. Jeon, J. Vac. Sci. Technol. B **32**, 06F505 (2014).
[12]Q. Dai, R. Guo, S.-Y. Lee, J. Choi, S.-H. Lee, I.-K. Shin, C.-U. Jeon, B.-G. Kim, and H.-K. Cho, Microelectron. Eng. **127**, 86 (2014).
[13]K. Suzuki, J. Shears, and B. Smith, *Microlithography: Science and Technology* (Marcel Dekker, New York, 1998).
[14]X. Zhao, S.-Y. Lee, J. Choi, S.-H. Lee, I.-K. Shin, C.-U. Jeon, B.-G. Kim, and H.-K. Cho, Microelectron. Eng. **133**, 78 (2015).

Redistribution subject to AVS license or copyright; see http://scitation.aip.org/termsconditions. IP: 131.204.73.184 On: Thu, 07 Apr 2016 01:29:43